crystals

MDPI

Article

Fabrication of Nano-Micro Hybrid Structures by Replication and Surface Treatment of Nanowires

Yeonho Jeong [1], Seunghang Shin [1], Hyunmin Choi [1], Seonjun Kim [1], Jihoon Kim [1], Sin Kwon [2], Kwang-Young Kim [2], Seung-Hyun Lee [2], Yoon-Gyo Jung [1] and Young Tae Cho [1,*]

[1] Department of Mechanical Engineering, Changwon National University, 20, Changwondaehak-ro, Uichang-gu, Changwon-si, Gyeongsangnam-do 51140, Korea; koriaj@naver.com (Y.J.); wsh9108@naver.com (S.S.); gusals3131@naver.com (H.C.); qdkman@naver.com (S.K.); jihoon2114@naver.com (J.K.); ygjung@changwon.ac.kr (Y.-G.J.)

[2] Department of Printed Electronics, Korea Institute of Machinery and Materials, Daejeon 34103, Korea; skwon@kimm.re.kr (S.K.); kwkim@kimm.re.kr (K.-Y.K.); shlee@kimm.re.kr (S.-H.L.)

* Correspondence: ytcho@changwon.ac.kr; Tel.: +82-55-213-3608

Academic Editor: Arkady Zhukov
Received: 16 June 2017; Accepted: 7 July 2017; Published: 11 July 2017

Abstract: Nanowire structures have attracted attention in various fields, since new characteristics could be acquired in minute regions. Especially, Anodic Aluminum Oxide (AAO) is widely used in the fabrication of nanostructures, which has many nanosized pores and well-organized nano pattern. Using AAO as a template for replication, nanowires with a very high aspect ratio can be fabricated. Herein, we propose a facile method to fabricate a nano-micro hybrid structure using nanowires replicated from AAO, and surface treatment. A polymer resin was coated between Polyethylene terephthalate (PET) and the AAO filter, roller pressed, and UV-cured. After the removal of aluminum by using NaOH solution, the nanowires aggregated to form a micropattern. The resulting structure was subjected to various surface treatments to investigate the surface behavior and wettability. As opposed to reported data, UV-ozone treatment can enhance surface hydrophobicity because the UV energy affects the nanowire surface, thus altering the shape of the aggregated nanowires. The hydrophobicity of the surface could be further improved by octadecyltrichlorosilane (OTS) coating immediately after UV-ozone treatment. We thus demonstrated that the nano-micro hybrid structure could be formed in the middle of nanowire replication, and then, the shape and surface characteristics could be controlled by surface treatment.

Keywords: anodic aluminum oxide; nanowires; UV nano imprint lithography; surface treatment

1. Introduction

Nanoscale structures such as nanoparticles, nanowires, nanopillars, and nanotubes have attracted attention because of their hidden characteristics in minute regions in various fields such as electricity, electronics, bio surfaces, and optics [1–8]. Among the nano-sized structures, nanowires can be used for stretchable and transparent electrodes [9], wearable sensors [10,11], interconnections [12,13], and nano-optics applications [14]. Nanoscale structures can be fabricated by various methods such as sol–gel methods, self-assembly, lithography and replication [15–20]. Among these, direct replication using a template is relatively easy, cost-effective, and applicable to various curable materials [21–26]. Anodic aluminum oxide (AAO) is widely used as a template for nanoscale structures since it has a large number of nanosized pores and micro-size height, which enable the fabrication of nanowires and nanotubes with a high aspect ratio [27–30]. However, at such a high aspect ratio, the nanowires are entangled due to the surface tension between them [31–33]. According to previous research, if the aspect ratio exceeds 15:1 when replicating with the AAO template, the nanowires do not stand upright

on the polymer film, but collapse and then clumped densely with each other. On the other hand, nanowires fabricated at an aspect ratio as low as 5:1 form, non-aggregated patterns [33,34]. Upon the removal of alumina using an etchant, the capillary force and surface tension play very important roles in the formation of nanowires. When the aspect ratio is high, the nanowires pull one another due to the surface tension, thereby aggregating together very easily. This aggregation occurs not only in polymer nanowires but also in metal nanowires. Many studies have attempted to prevent such aggregation [35], two approaches have been proposed. One involves hydration of the nanowire surface, which can decrease the agglomeration due to surface tension when the liquid filled in the spaces among the nanowires evaporates. The other involves freeze-drying removal, which suppresses the flow of the etchant, so that the force produced by surface tension between the nanowires is decreased.

Despite various efforts, straightening nanowires with a high aspect ratio remains a challenge. In this study, we attempted to fabricate nano-micro hybrid structures from tangled high-aspect-ratio nanowires by exploiting the aggregation phenomenon in a positive manner. The structure can be changed by adjusting various parameters during the manufacture of nanowires. In addition, the behavior of micropatterns with tangled nanowires and surface wettability were investigated after surface treatment. The nanowire structure fabricated using the AAO filter and polyurethane-acrylate (PUA) type resins with viscosities of 257.4 cPs and 7.2 cPs were tested. UV nano imprint lithography (UV-NIL) was applied, and AAO was etched with the help of NaOH solution. In addition, a self-assembled monolayer coating and UV ozone treatment were applied. The shape of the nano-micro hybrid structure was determined by SEM images, and the surface characteristics were investigated by contact angle measurements [36,37].

2. Aggregation of Nanowires

2.1. Fabrication of Nanowire Structure

Figure 1a shows a schematic of the nano-imprint process used in this experiment. Nanowires were fabricated by replication using a porous template referred to as AAO filter (Whatman, anodisc 25, average diameter of 200 nm, thickness of 60 μm, Figure 2b). After cleaning the PET film using isopropyl alcohol (IPA) and acetone, a UV-curable PUA-type resin was dropped and coated on the PET substrate with the help of a spin coater. Two types of resins with different viscosities, 257.4 cPs and 7.2 cPs, were examined. The AAO filter contacts were sequentially and pressed by a roller, as shown in Figure 1d. While maintaining contact, the pressing force was released and UV light was irradiated for a sufficient time (around 30 s). Then, instead of physical demolding, the cured material was immersed in 2 mol of NaOH etchant for 10 min for complete removal of the AAO filter, rinsed with deionized (DI) water, and dried using an air gun [38]. The etching time and rinsing method were confirmed by energy dispersive X-ray (EDX) analysis when there was no residue of Na and Al. Since the thickness of the AAO filter was 60 μm and pore diameter was 0.2 μm, the aspect ratio was 120:1, and the cured resin and AAO filter were very tightly attached. Therefore, the physical separation is totally impossible and if it is tried to demold with even weak forces, the AAO filter cannot but break. According to previous studies, etching can be performed using various etchants (NaOH, KOH and H_3PO_4) to remove the AAO filter [39–42]. We tested 2 mol of each etchant for the same etching time. Among the solutions tested, the NaOH solution showed the highest etching rate because of its superior ability to penetrate nanosized spaces. Figure 1c shows the fabricated polymer nanowire on the PET film. The structure was investigated by SEM observations of the surface and cross-section.

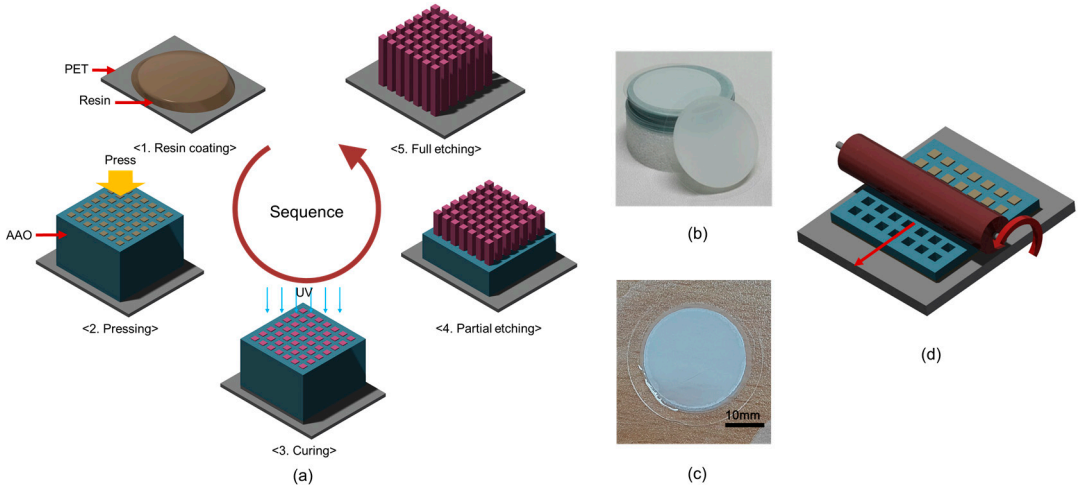

Figure 1. (**a**) Nanowire fabrication by nano imprinting with soluble aluminum oxide; (**b**) AAO filters; (**c**) Replicated nanowire pattern on PET film; (**d**) Roller pressing for nano imprint process.

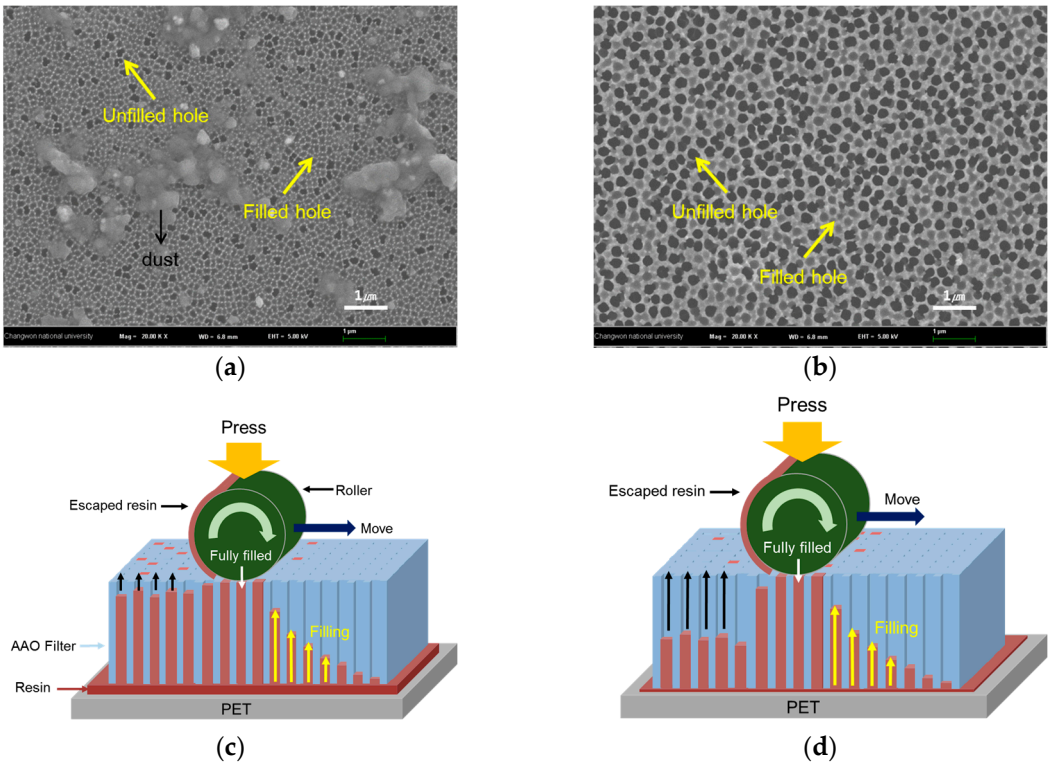

Figure 2. Surface of AAO filter with cured polymer resins before etching (×20,000); (**a**) viscosity 257.4 cPs; (**b**) viscosity 7.2 cPs; Schematic for explanation of resin filling in the holes of AAO after roller pressing: (**c**) higher viscosity; (**d**) lower viscosity.

2.2. Changes in Nanowire Structure with Viscosity of Resin

Figure 2a,b denote the top surface of the AAO filter with the cured polymer resin before etching. We used resins with two different viscosities of 257.4 cPs and 7.2 cPs; in each case, they had different structures. In these figures, filled and unfilled holes were observed; a greater number of unfilled holes could be seen on the surface of the AAO filter with the cured polymer when the low-viscosity resin was used. This interesting phenomenon can be explained by the schematics in Figure 2c,d. The resin coated on the PET film goes up by the capillary force and is squeezed by roller pressing; then, the holes

are fully filled with the resin and some of the ones touching the roller are escaped out again. When using the low-viscosity resin, a large amount of resin escaped from the holes because of the weaker cohesion force as compared to that for the high-viscosity resin (Figure 2c). The difference between the filled and unfilled holes would result in a difference in the height of the micropatterns, as mentioned later in the text.

Nanowires with a high aspect ratio have a higher curvature and tend to agglomerate. Research on these phenomena has been conducted extensively, and when the etched alumina solution is removed, the surface tension and capillary forces act on the nanowires, resulting in aggregation [33,43]. As schematically detailed in Figure 3, the aggregated nanowires will form a micropattern, and the size of the pattern will vary depending on the type of resin. This structure can be regarded as a nano-micro hybrid structure because the micropattern is composed of nanopatterns. Figure 4 shows the top and cross-sectional view of the fabricated nano-micro hybrid structure with aggregated nanowires. Hill and valley shapes can be seen in the cross-sectional view. The micropattern formed by the tangled and aggregated nanowires is a type of hole that is approximately 40–50 μm height and 25–35 μm in diameter.

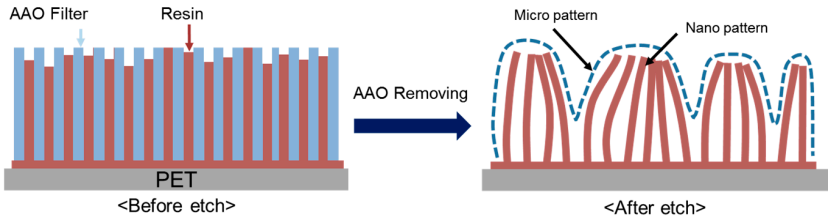

Figure 3. Schematic for fabrication of nano-micro hybrid patterns by aggregation of nanowires after complete etching.

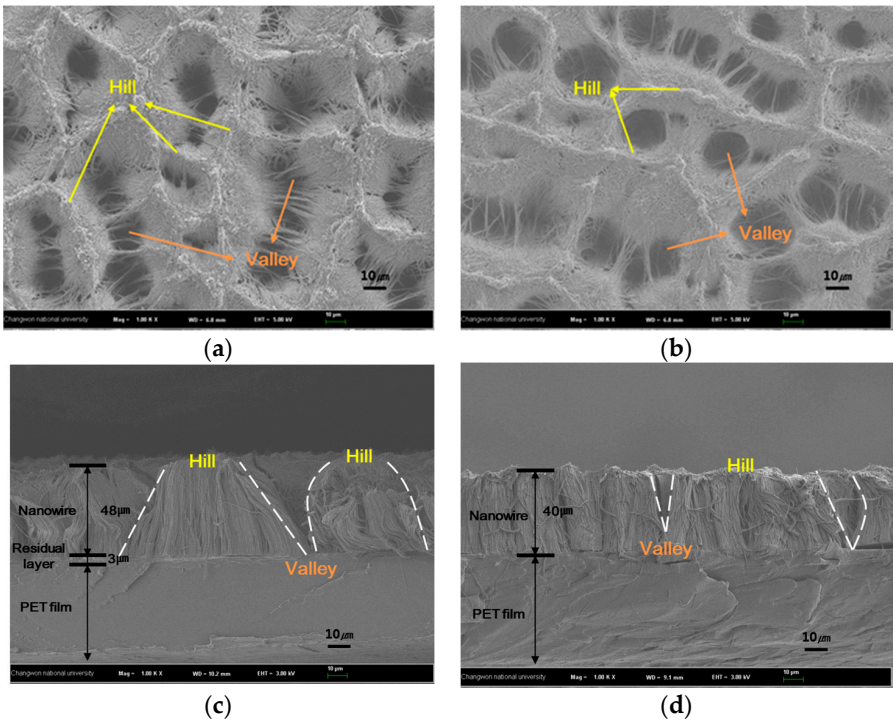

Figure 4. Fabricated nano-micro hybrid structure with aggregated nanowires after full etching (×1000). (**a**) Surface of the structure with viscosity 257.4 cPs; (**b**) Surface of the structure with viscosity 7.2 cPs; (**c**) Cross-section of the structure with viscosity 257.4 cPs; (**d**) Cross-section of the structure with viscosity 7.2 cPs.

Experiments on the two resins with different viscosities revealed that the overall shape of the patterns is similar, but the height of the patterns is clearly different. A thicker nanowire layer is observed when using the high-viscosity resin than when using the low-viscosity resin (Figure 4c,d), because of the longer wires obtained in the former case.

3. Effect of Surface Treatment

3.1. Variation of Wettability with Surface Treatment

We investigated the change in the surface formation and properties when various surface treatments were performed on the fabricated nano-micro hybrid structure. One of the surface treatments carried out in experiments is self-assembled monolayers (SAMs) coating with OTS, which is considered to have hydrophobic properties, and the other is UV-ozone treatment known as hydrophilic treatment [44,45]. In SAMs coating, the surface is modified via the formation of an organic molecule film spontaneously aligned on the surface [44,46]. In this experiment, the fabricated nano-micro hybrid patterns were coated by a vapor deposition technique using OTS (Sigma-Aldrich) in which a long hydrocarbon chain is bonded to trichlorosilane. 10 mL of the OTS coating solution was placed in a beaker on the hot plate inside a glove box where a N_2 atmosphere is maintained. The hot plate was kept at 100 °C and the fabricated surface was exposed to the vapor for 60 min. In UV-ozone treatment, ozone (O_3) is generated by irradiation of a strong oxidizing power with ultraviolet rays. The ozone that is produced oxidizes, decomposes, and removes the organic matter on the glass, film, and metal surface, and reforms the surface of the material, resulting in hydrophobic or hydrophilic patterns [45,47,48]. Ultraviolet rays having a wavelength of 185 nm to 254 nm were focused on the surface for 60 min.

Before surface treatments of the fabricated entangled nanowires, the characteristics of each surface treatment were examined on the flat cured PUA-type resin without patterns. After each surface treatment was carried out, the contact angle was measured by dropping 5 μL of DI water on the surface, as shown in Figure 5. Without any treatment, that is, when the material was just cured, the contact angle was about 90°, which indicates the inherent surface energy of the material. Figure 5b shows the contact angle after OTS coating with silan monolayer. The contact angle increased by about 10°, and from this result, it can be clearly seen that the OTS coating makes the surface state hydrophobic. On the other hand, the contact angle was measured to be as small as 31° after the UV-ozone treatment as shown in Figure 5c. That is, the wettability of the surface can be improved, so this can be said to be a hydrophilic treatment.

There have been many studies on the effect of increasing amounts of oxygen on the surface subjected to UV-ozone treatment, and the surface energy is reported to change accordingly [46–48]. Also, a study focused on how the shape of Pt nanoparticles is affected by UV-ozone treatment [49]. Based on the previous studies, a preliminary experiment on UV-ozone treatment was conducted using cylindrical micropatterns with a diameter of 5 μm and a height of 10 μm. Cylinder patterns with nanosized rugged surfaces were fabricated by UV-NIL using the PUA polymer, as shown in Figure 6a. After UV-ozone treatment for 60 min, the rough surface became smooth, as shown in Figure 6b. Excessive UV energy can produce even cracks on the surface of the polymer pattern. Due to the smoothing effect, the diameter of the cylinder structure decreased from 5 μm to 4.2 μm. From this result, it can be concluded that the polymer structure becomes smooth when exposed to UV-ozone for a long time. In particular, nanowire structures are very susceptible to the smoothening effect.

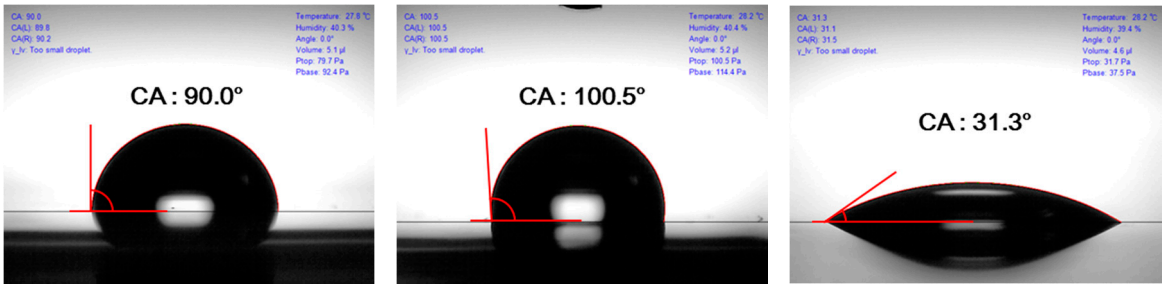

(**a**) (**b**) (**c**)

Figure 5. Contact angle of the cured polymer surface with PUA resin after various surface treatments: (**a**) before surface treatment and after (**b**) OTS coating and (**c**) UV-ozone treatment.

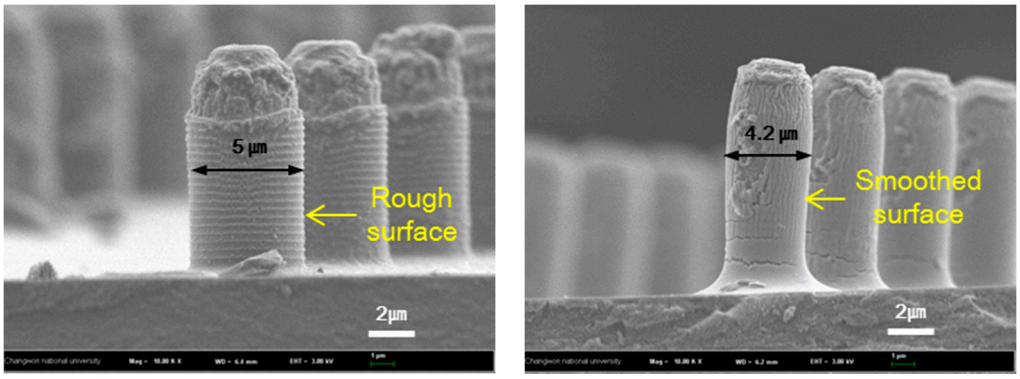

(**a**) (**b**)

Figure 6. The change in the polymer structures following UV-ozone treatment. (**a**) Fabricated polymer structures; (**b**) The structures after UV-ozone treatment for 60 min.

3.2. Structure Variation with Surface Treatments

Two representative types of surface treatments mentioned above were carried out on the nano-micro hybrid structure formed by nanowires, to investigate the change in surface characteristics. Figure 7 shows the surface and cross section of the nano-micro hybrid structure after OTS coating. Since silan monolayer is coated on the surface, its shape is similar to that of the structure before surface treatment. Dimple structures appear relatively uniformly throughout the entire surface. The diameter of each dimple was about 30 ± 5 μm as shown in Figure 7b. The cross section shows that the tangled nanowires maintain their shape to the tip. Although a 60-μm-thick AAO filter was used, the thickness of the nanowire layer was about 50 μm since the nanowires were tangled together to form a dimple structure. However, UV-ozone treatment on the tangled-nanowire micro structure greatly changed the surface state. The size of dimples was approximately two times larger on average as shown in Figure 8b. Moreover, additional shapes like bumpy structures appeared in some locations. As the ends of the nanowires exposed to UV-ozone melted together, a smooth surface was formed. Figure 8d clearly shows the cross section of this bumpy structures and smoothed parts.

In addition, we tried both surface treatments sequentially. Figure 9 shows the top and cross-sectional surface after UV-ozone treatment followed by OTS coating. The OTS coating did not affect the shape of the surface, whereas the UV-ozone affected the shape, so the final shape after this double treatment was similar to that after UV-ozone treatment alone.

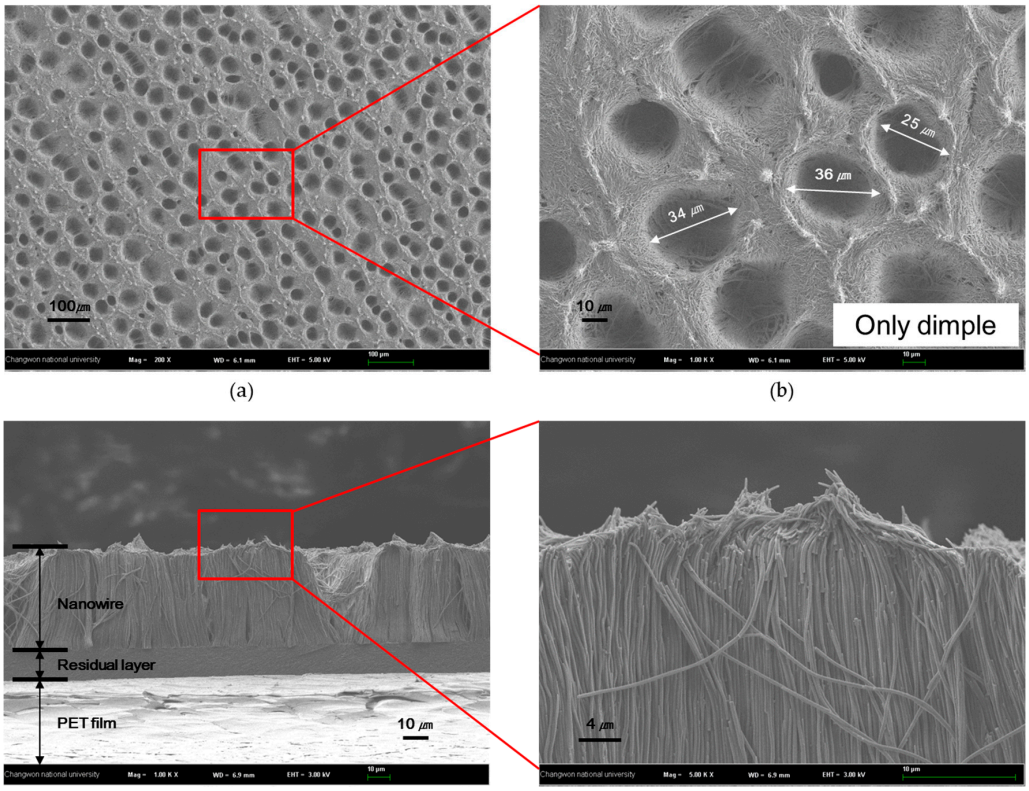

Figure 7. Nano-micro hybrid structures with OTS coating: (**a**) Surface (×200); (**b**) surface (×1000); (**c**) cross section (×1000); and (**d**) cross section (×5000).

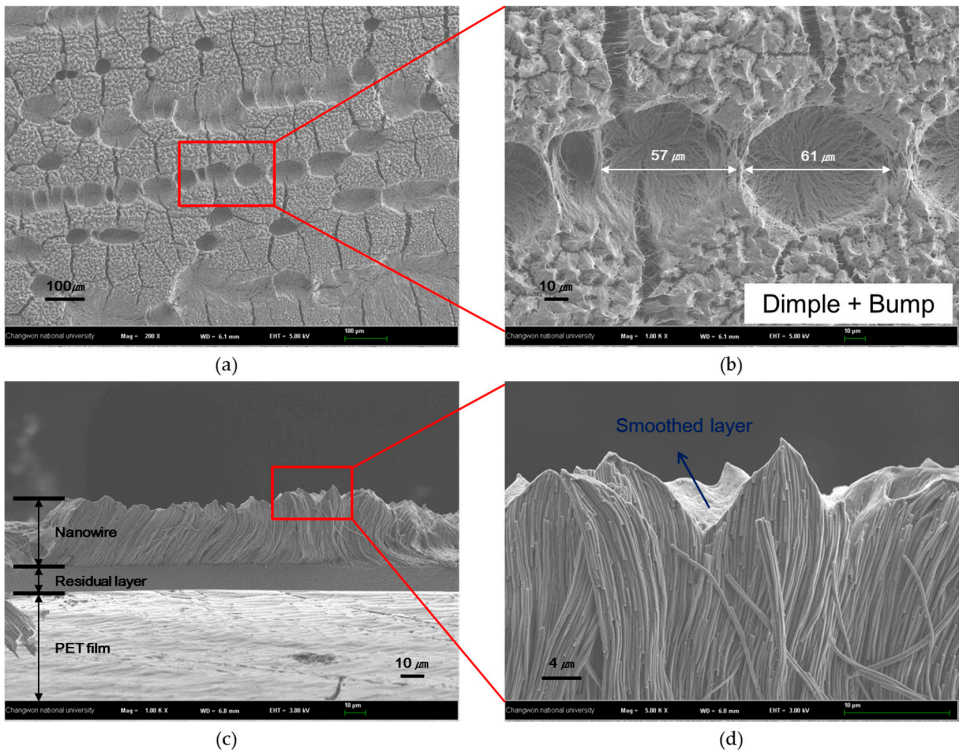

Figure 8. Nano-micro hybrid structures with UV-ozone treatment: (**a**) Surface (×200); (**b**) surface (×1000); (**c**) cross section (×1000); and (**d**) cross section (×5000).

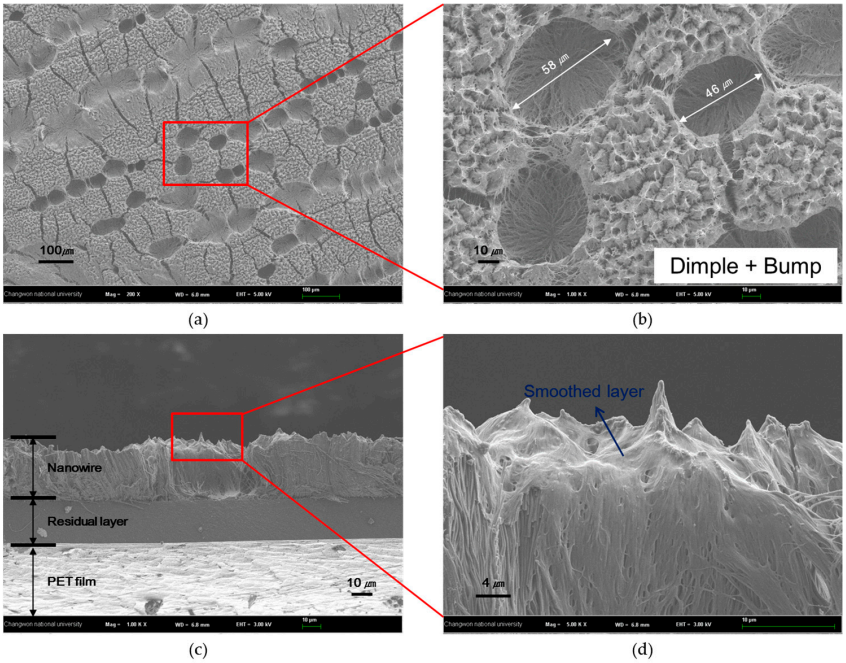

Figure 9. Nano-micro hybrid structures with double surface treatments: (**a**) Surface (×200); (**b**) surface (×1000); (**c**) cross section (×1000); and (**d**) cross section (×5000).

3.3. Contact Angle Variation with Surface Treatment

In order to investigate the wettability of the surfaces according to various surface treatments, the contact angle was measured. The contact angle with non-before surface treatments could not be measured, because the dropped water was absorbed into the nano-micro hybrid pattern as soon as it came in contact with the surfaces. In this case, the surface was super-hydrophilic.

The contact angle measurement results after surface treatment are shown in Figure 10. After the OTS coating, the contact angle was measured to be about 117 ± 4° (Figure 10a). The super-hydrophilic entangled-nanowire surface with microsized dimples becomes water-repellent even with OTS coating alone. The contact angle after UV-ozone treatment was measured to be about 127 ± 3° (Figure 10b). It is a peculiar phenomenon that the contact angle after UV-ozone treatment is higher than that after OTS coating. The reason for this is considered to be the fact that the effect of the formation of a nano-micro hybrid structure having an appropriate size is greater than the effect of the formation of the silane monolayer on the surface to impart hydrophobicity. In order to enhance the hydrophobicity, OTS coating was conducted after UV-ozone treatment and the measured value was about 134 ± 3° (Figure 10c). The monolayer was coated on the properly formed nano-micro hybrid structure, so this double treated surface had the highest hydrophobicity.

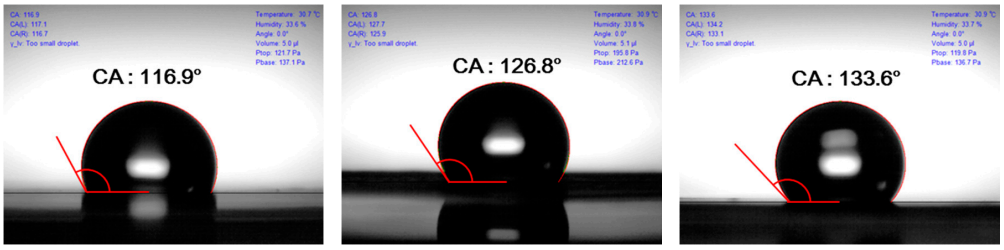

Figure 10. Contact angles with the nano-micro hybrid structures after various surface treatments: (**a**) OTS coating; (**b**) UV-ozone treatment; and (**c**) OTS coating after UV-ozone treatment.

4. Conclusions

The nanowire structure was fabricated via a UV nano imprint process using an AAO filter as a template. It was revealed that nanowires aggregated together to form a micropattern after the alumina etching process. Surface treatments, i.e., OTS coating and UV-ozone treatment were conducted on the fabricated nano-micro hybrid surface, and the structural change and surface variations are investigated.

The phenomenon of nanowire aggregation was investigated when nanowires were fabricated using polymer-type UV resins. The shapes of the nano-micro hybrid structure after full etching with different resins were similar. However, the length of nanowires of the resin with 257.4 cPs was longer; this is because the residual resin filled voids because of capillary force under pressure. However, the resin with 7.2 cPs could not be filled in voids, because there was no residual resin. Therefore, the amounts of filled resin differed.

The behaviors and surface wettability of nanowires after the OTS coating and UV-ozone treatment on the surface of the fabricated structure were investigated. There were only dimple structures after the aggregated nanowires were formed, but bump structures appeared after UV-ozone treatment because of the smoothed surface. Further, the size of the dimple increased to about 60 $\pm$ 10 μm after UV-ozone treatment. The nano-micro hybrid structure without surface treatments showed a super-hydrophilic behavior because the water permeated into spaces between the uncoated nanowires. When the silane monolayer was coated on this surface with the hybrid structure, a contact angle of about 117 $\pm$ 2° was obtained, but the surface got wet gradually. Further, the surface with the composite structure was subjected to UV-ozone treatment, and a contact angle of about 127 $\pm$ 3° was obtained. This phenomenon is because the top part of the composite structure coated with the silane monolayer is cured after smoothening, so water molecules could not be permeated between the structures, thus forming nano-micro hybrid structures. After the double treatment was carried out, the surface structure showed the same shape as when UV-ozone treatment was performed. The surface contact angle was 134 $\pm$ 2° or more, which indicates that a monomolecular layer formed on the surface as a result of UV-ozone treatment, and a higher contact angle was obtained. By using the fabricated composite structure, it is possible to fabricate a composite structure of embossing when duplicating again, and it is possible to form a hybrid pattern. Study results are summarized in Tables 1 and 2.

Table 1. Results for the fabrication of nano-micro hybrid structures using the AAO filter with different viscosities of PUA resins after full etching.

Viscosity of PUA Resins	Thickness of Nanowire Layer	Note
257.4 cPs	48 $\pm$ 4 μm	The resin with 257.4 cPs viscosity was well filled into AAO filter because of difference of cohesion force
7.2 cPs	40 $\pm$ 5 μm	

Table 2. Results of the fabrication of nano-micro hybrid structures according to surface treatments.

Surface Treatment	Contact Angle	Structure (The Size of Dimples)	Note
No treatment	Super hydrophilic	30 $\pm$ 5 μm	The nano-micro hybrid structure because of the aggregated nanowires was obtained
Silane monolayer treatment	117 $\pm$ 2°	Similar to that for no treatment	The hydrophobic surface was fabricated because silane monolayer was coated
UV-ozone treatment	127 $\pm$ 3°	60 $\pm$ 10 μm	The contact angle increased because of smoothed layer
Double treatment	134 $\pm$ 2°	Similar to that for UV-ozone treatment	The contact angle was higher according to the silane monolayer

Acknowledgments: This research was supported by the Ministry of Trade, Industry & Energy (MOTIE), Korea Institute for Advancement of Technology (KIAT) through the Encouragement Program for The Industries of Economic Cooperation Region and was supported by the Basic Science Research Program through the National Research Foundation of Korea (NRF) funded by the Ministry of Science, ICT & Future Planning (NRF-2017R1A2B4008053).

Author Contributions: Yeonho Jeong, Sin Kwon, Kwang-Young Kim, Seung Hyun Kim and Young Tae Cho conceived and designed the experiments; Yeonho Jeong, Seunghang Shin, Hyunmin Choim and Seonjun Kim performed the experiments; Seunghang Shin, Hynmin Choi and Young Tae Cho analyzed the data; Yeonho Jeong, Seunghang Shin, Hyunmin Choi and Jihoon Kim wrote the paper.

Conflicts of Interest: The authors declare no conflict of interest.

References

1. Elghanian, R.; Storhoff, J.J.; Mucic, R.C.; Letsinger, R.L.; Mirkin, C.A. Selective colorimetric detection of polynucleotides based on the distance-dependent optical properties of gold nanoparticles. *Science* **1997**, *277*, 1078–1081. [CrossRef] [PubMed]
2. Berdichevsky, Y.; Lo, Y.H. Polypyrrole nanowire actuators. *Adv. Mater.* **2016**, *18*, 122–125. [CrossRef]
3. Mitchell, D.T.; Lee, S.B.; Trofin, L.; Li, N.; Nevanen, T.K.; Söderlund, H.; Martin, C.R. Smart nanotubes for bioseparations and biocatalysis. *J. Am. Chem. Soc.* **2002**, *124*, 11864–11865. [CrossRef] [PubMed]
4. Nicewarner-Pena, S.R.; Freeman, R.G.; Reiss, B.D.; He, L.; Peña, D.J.; Walton, I.D.; Cromer, R.; Keating, C.D.; Natan, M.J. Submicrometer metallic barcodes. *Science* **2001**, *294*, 137–141. [CrossRef] [PubMed]
5. Dersch, R.; Steinhart, M.; Boudriot, U.; Greiner, A.; Wendorff, J.H. Nanoprocessing of polymers: Applications in medicine, sensors, catalysis, photonics. *Polym. Adv. Technol.* **2005**, *16*, 276–282. [CrossRef]
6. Baker, L.A.; Jin, P.; Martin, C.R. Biomaterials and biotechnologies based on nanotube membranes. *Crit. Rev. Solid State Mater. Sci.* **2005**, *30*, 183–205. [CrossRef]
7. Xiang, H.; Shin, K.; Kim, T.; Moon, S.I.; McCarthy, T.J.; Russell, T.P. Block copolymers under cylindrical confinement. *Macromolecules* **2004**, *37*, 5660–5664. [CrossRef]
8. Fei, G.; Tuinea-Bobe, C.; Li, D.; Li, G.; Whiteside, B.; Coates, P.; Xia, H. Electro-activated surface micropattern tuning for microinjection molded electrically conductive shape memory polyurethane composites. *RSC Adv.* **2013**, *3*, 24132–24139. [CrossRef]
9. Kim, K.; Kim, J.; Hyun, B.G.; Ji, S.; Kim, S.Y.; Kim, S.W.; An, B.W.; Park, J.U. Stretchable and transparent electrodes based on in-plane structures. *Nanoscale* **2015**, *7*, 14577–14594. [CrossRef] [PubMed]
10. Kim, J.; Kim, M.; Lee, M.S.; Kim, K.; Ji, S.; Kim, Y.T.; Park, J.H.; Na, K.M.; Bae, K.H.; Kim, H.K.; et al. Wearable smart sensor systems integrated on soft contact lenses for wireless ocular diagnostics. *Nat. Commun.* **2017**, *8*, 14997. [CrossRef] [PubMed]
11. Park, J.; Kim, J.; Kim, K.; Kim, S.Y.; Cheong, W.H.; Park, K.; Song, J.H.; Namgoong, G.; Kim, J.J.; Heo, J.; et al. Wearable, wireless gas sensors using highly stretchable and transparent structures of nanowires and graphene. *Nanoscale* **2016**, *8*, 10591–10597. [CrossRef] [PubMed]
12. An, B.W.; Kim, K.; Lee, H.; Kim, S.Y.; Shim, Y.; Lee, D.Y.; Song, J.Y.; Park, J.U. High-resolution printing of 3D structures using an electrohydrodynamic inkjet with multiple functional inks. *Adv. Mater.* **2015**, *27*, 4322–4328. [CrossRef] [PubMed]
13. Kim, M.; Park, J.; Ji, S.; Shin, S.H.; Kim, S.Y.; Kim, Y.C.; Kim, J.Y.; Park, J.U. Fully-integrated, bezel-less transistor arrays using reversibly foldable interconnects and stretchable origami substrates. *Nanoscale* **2016**, *8*, 9504–9510. [CrossRef] [PubMed]
14. Zhao, Y.S.; Zhan, P.; Kim, J.; Sun, C.; Huang, J. Patterned growth of vertically aligned organic nanowire waveguide arrays. *ACS Nano* **2010**, *4*, 1630–1636. [CrossRef] [PubMed]
15. Kuo, C.W.; Shiu, J.Y.; Chen, P. Size-and shape-controlled fabrication of large-area periodic nanopillar arrays. *Chem. Mater.* **2003**, *15*, 2917–2920. [CrossRef]
16. Lee, S.B.; Koepsel, R.; Stolz, D.B.; Warriner, H.E.; Russell, A.J. Self-assembly of biocidal nanotubes from a single-chain diacetylene amine salt. *J. Am. Chem. Soc.* **2004**, *126*, 13400–13405. [CrossRef] [PubMed]
17. Gibson, J.M. Reading and writing with electron beams. *Phys. Today* **1997**, *50*, 56–61. [CrossRef]
18. Kramer, N.; Birk, H.; Jorritsma, J.; Schönenberger, C. Fabrication of metallic nanowires with a scanning tunneling microscope. *Appl. Phys. Lett.* **1995**, *66*, 1325–1327. [CrossRef]

19. Jiang, P.; Bertone, J.F.; Colvin, V.L. A lost-wax approach to monodisperse colloids and their crystals. *Science* **2001**, *291*, 453–457. [CrossRef] [PubMed]
20. Steinhart, M.; Wendorff, J.H.; Greiner, A.; Wehrspohn, R.B.; Nielsch, K.; Schilling, J.; Choi, J.; Gösele, U. Polymer nanotubes by wetting of ordered porous templates. *Science* **2002**, *296*, 1997. [CrossRef] [PubMed]
21. Hong, S.H.; Hwang, J.; Lee, H. Replication of cicada wing's nano-patterns by hot embossing and UV nanoimprinting. *Nanotechnology* **2009**, *20*, 385303. [CrossRef] [PubMed]
22. Han, K.S.; Shin, J.H.; Yoon, W.Y.; Lee, H. Enhanced performance of solar cells with anti-reflection layer fabricated by nano-imprint lithography. *Sol. Energy Mater. Sol. Cells* **2011**, *95*, 288–291. [CrossRef]
23. Choo, S.; Choi, H.J.; Lee, H. Replication of rose-petal surface structure using UV-nanoimprint lithography. *Mater. Lett.* **2014**, *121*, 170–173. [CrossRef]
24. Yu, Z.; Chou, S.Y. Triangular profile imprint molds in nanograting fabrication. *Nano Lett.* **2004**, *4*, 341–344. [CrossRef]
25. Hirai, Y.; Harara, S.; Isaka, S.; Kobayashi, M.; Tanaka, Y. Nano-Imprint lithography using replicated mold by Ni electroforming. *Jpn. J. Appl. Phys.* **2002**, *41*, 4186. [CrossRef]
26. Kim, J.H.; Cho, Y.T.; Jung, Y.G. Selection of absorptive materials for non-reflective wire grid polarizers. *Int. J. Precis. Eng. Manuf.* **2016**, *17*, 903–908. [CrossRef]
27. Stępniowski, W.J.; Salerno, M. Fabrication of nanowires and nanotubes by anodic alumina template-assisted electrodeposition. *Manuf. Nanostruct.* **2014**, *12*, 321–357.
28. Sousa, C.T.; Leitao, D.C.; Proenca, M.P.; Ventura, J.; Pereira, A.M.; Araujo, J.P. Nanoporous alumina as templates for multifunctional applications. *Appl. Phys. Rev.* **2014**, *1*, 031102. [CrossRef]
29. Hong, S.H.; Bae, B.J.; Lee, H.; Jeong, J.H. Fabrication of high density nano-pillar type phase change memory devices using flexible AAO shaped template. *Microelectron. Eng.* **2010**, *87*, 2081–2084. [CrossRef]
30. Schwirn, K.; Lee, W.; Hillebrand, R.; Steinhart, M.; Nielsch, K.; Gösele, U. Self-ordered anodic aluminum oxide formed by H_2SO_4 hard anodization. *ACS Nano* **2008**, *2*, 302–310. [CrossRef] [PubMed]
31. Lee, P.S.; Lee, O.J.; Hwang, S.K.; Jung, S.H.; Jee, S.E.; Lee, K.H. Vertically aligned nanopillar arrays with hard skins using anodic aluminum oxide for nano imprint lithography. *Chem. Mater.* **2005**, *17*, 6181–6185. [CrossRef]
32. Lopes, M.C.; de Oliveira, C.P.; Pereira, E.C. Computational modeling of the template-assisted deposition of nanowires. *Electrochim. Acta* **2008**, *53*, 4359–4369. [CrossRef]
33. Choi, M.K.; Yoon, H.; Lee, K.; Shin, K. Simple fabrication of asymmetric high-aspect-ratio polymer nanopillars by reusable AAO templates. *Langmuir* **2011**, *27*, 2132–2137. [CrossRef] [PubMed]
34. Kim, Y.S.; Lee, K.; Lee, J.S.; Jung, G.Y.; Kim, W.B. Nanoimprint lithography patterns with a vertically aligned nanoscale tubular carbon structure. *Nanotechnology* **2008**, *19*, 365305. [CrossRef] [PubMed]
35. Chen, G.; Soper, S.A.; McCarley, R.L. Free-standing, erect ultrahigh-aspect-ratio polymer nanopillar and nanotube ensembles. *Langmuir* **2007**, *23*, 11777–11781. [CrossRef] [PubMed]
36. Choi, W.K.; Kim, S.H.; Choi, S.G.; Lee, E.S.; Lee, C.H. Effect of pad's surface deformation and oscillation on monocrystalline silicon wafer surface quality. *Int. J. Precis. Eng. Manuf.* **2014**, *15*, 2301–2307. [CrossRef]
37. Schonhorn, H.; Hansen, R.H. Surface treatment of polymers for adhesive bonding. *J. Appl. Polym. Sci.* **1967**, *11*, 1461–1474. [CrossRef]
38. Liang, Y.; Zhen, C.; Zou, D.; Xu, D. Preparation of free-standing nanowire arrays on conductive substrates. *J. Am. Chem. Soc.* **2004**, *126*, 16338–16339. [CrossRef] [PubMed]
39. Hu, G.; Zhang, H.; Di, W.; Zhao, T. Study on wet etching of AAO template. *Appl. Phys. Res.* **2009**, *1*, 78–82. [CrossRef]
40. Song, G.; Chen, D.; Peng, Z.; She, X.; Li, J.; Han, P. Quantificational etching of AAO template. *J. Mater. Sci. Technol. Shenyang* **2007**, *23*, 427.
41. Murphy, A.; McPhillips, J.; Hendren, W.; McClatchey, C.; Atkinson, R.; Wurtz, G.; Zayats, A.V.; Pollard, R.J. The controlled fabrication and geometry tunable optics of gold nanotube arrays. *Nanotechnology* **2010**, *22*, 045705. [CrossRef] [PubMed]
42. Gu, D.; Baumgart, H.; Abdel-Fattah, T.M.; Namkoong, G. Synthesis of nested coaxial multiple-walled nanotubes by atomic layer deposition. *ACS Nano* **2010**, *4*, 753–758. [CrossRef] [PubMed]
43. Chu, C.W.; Huang, Y.C.; Tsai, C.C.; Chen, J.T. Wetting in nanopores of cylindrical anodic aluminum oxide templates: Production of gradient polymer nanorod arrays on large-area curved surfaces. *Eur. Polym. J.* **2015**, *63*, 141–148. [CrossRef]

44. Lim, S.C.; Kim, S.H.; Lee, J.H.; Kim, M.K.; Zyung, T. Surface-treatment effects on organic thin-film transistors. *Synth. Met.* **2005**, *148*, 75–79. [CrossRef]
45. Gongjian, B.; Yunxuan, W.; Xingzhou, H. Surface modification of polyolefine by UV light/ozone treatment. *J. Appl. Polym. Sci.* **1996**, *60*, 2397–2402. [CrossRef]
46. Maoz, R.; Matlis, S.; DiMasi, E.; Ocko, B.M.; Sagiv, J. Self-replicating amphiphilic monolayers. *Nature* **1996**, *384*, 150. [CrossRef]
47. Nie, H.Y.; Walzak, M.J.; Berno, B.; McIntyre, N.S. Atomic force microscopy study of polypropylene surfaces treated by UV and ozone exposure: Modification of morphology and adhesion force. *Appl. Surf. Sci.* **1999**, *144*, 627–632. [CrossRef]
48. Efimenko, K.; Wallace, W.E.; Genzer, J. Surface modification of Sylgard-184 poly (dimethyl siloxane) networks by ultraviolet and ultraviolet/ozone treatment. *J. Colloid Interface Sci.* **2002**, *254*, 306–315. [CrossRef] [PubMed]
49. Vidal-Iglesias, F.J.; Solla-Gullón, J.; Herrero, E.; Montiel, V.; Aldaz, A.; Feliu, J.M. Evaluating the ozone cleaning treatment in shape-controlled Pt nanoparticles: Evidences of atomic surface disordering. *Electrochem. Commun.* **2001**, *13*, 502–505. [CrossRef]